Journal of Machine Engineering, 2024, Vol. 24, No.2, 117-128
ISSN 1895-7595 (Print) ISSN 2391-8071 (Online)

Received*: 29 February 2024* / Accepted: *06 May 2024* / Published online: *13 May 2024*

wire arc additive manufacturing,
cold metal transfer,
wire feed speed sensivity,
thermofluid model

Alizee REMY[1,2*],
Uzoma-Vincent NWANKPA[1,2],
Matthieu RAUCH[1,2],
Jean-Yves HASCOET[1,2],
Guillaume RUCKERT[2,3]

IMPACT OF A VARIATION IN WIRE FEED SPEED ON DEPOSITS FROM THE WIRE ARC ADDITIVE MANUFACTURING (WAAM)

Metal Additive Manufacturing (MAM) is one of the innovative industrial technologies of the last decade, which presents some benefits as compared to traditional manufacturing techniques. MAM is faster, less expensive, and allow the manufacturing of large, complex components than casting, foundry etc. Understanding the influence of process parameters on the deposited matter and material characteristics is essential for the manufacturing of industrial parts. Current research concentrates on the impact of parameters on the fabricated structure geometry, microstructure and mechanical properties. There are limited number of studies, that focus on the possibility of Wire Feed Speed (WFS) parameter variation during deposition. In this work, a series of trials were realised with Cold Metal Transfer. The results showed that the quantity of material deposited was lesser than the theoretical value. The variation obtained was explained by the difference between the inputted WFS on the generator and the actual WFS output. Hence, the result on the influence of the variation of WFS on bead geometry was applied to a thermofluid model with Ti-6Al-4V alloy to confirm the sensitivity of this parameter in the quantity and geometry of the material deposited.

1. INTRODUCTION

Metal Additive Manufacturing (MAM) was developed for many industrial applications in the last decade where by large components are manufactured by depositing molten metal in a layer by layer fashion. MAM proffers a lot of advantages in the manufacturing industry such as reduction in material wastage [1], optimisation and manufacturing of part with complex geometries, and reduction of lead time [2]. MAM are capable of giving mechanical

[1] Nantes Université, École Centrale Nantes, CNRS, GeM, UMR6183, F-44000 Nantes, France
[2] Additive Manufacturing Group, Joint Laboratory of Marine Technology (JLMT) Centrale Nantes,–Naval Group, France
[3] Naval Group - DT/ MET/CESMAN, - Technocampus Ocean 5 rue de l'Halbrane 44340 Bouguenais, France
[*] E-mail: alizee.remy@ec-nantes.fr
https://doi.org/10.36897/jme/188308

properties similar to parts made by traditional means. A wide variety of applications are exploited in the industry because of these advantages [3]. Currently, parts produced by additive manufacturing are being implemented in the medical, aerospace, aeronautical, and naval fields [4]. Wire Arc Additive Manufacturing (WAAM) is a type of MAM which uses arc as heat source to melt the fed metallic wire in fabrication of a 3D part.

There are several heat sources used for WAAM, Metal Tungsten inert gas (TIG), Plasma arc welding (PAW) and Metal inert gas (MIG). TIG and Plasma are precise process that produce an electrical arc with a non-consumable tungsten electrode. They rely on inert shielding gas to protect the weld area from atmospheric contamination. In addition, Plasma process has a constricted arc and higher energy density. They are known for producing high-quality welds with minimal spatter [5,6]. MIG welding is the most common heat source due to its utilization of a direct feeding spool of welding wire, which is coaxial with the welding torch and has high deposition rate [5]. Cold metal transfer (CMT), is a variant of MIG, which was introduced and patented by Fronius [9]. The metal droplet transfer in CMT is done by a push-pull system, which mechanically retract the wire during short circuit without relying on electromagnetic force [9]. Hence, the arc remains stable regardless of the surface being welded or the speed of joining, enabling the utilization of the CMT welding technique in any position and for various applications [7,8]. CMT is known as a low heat input process, and can be operated in various mode such as CMT advanced, CMT pulse advanced and CMT pulse [7,8]. CMT+P combines CMT with a pulsed arc, where an extra droplet is deposited in each cycle enhancing the deposition rate, [9]. The equipment generally used for WAAM process is shown in Fig. 1.

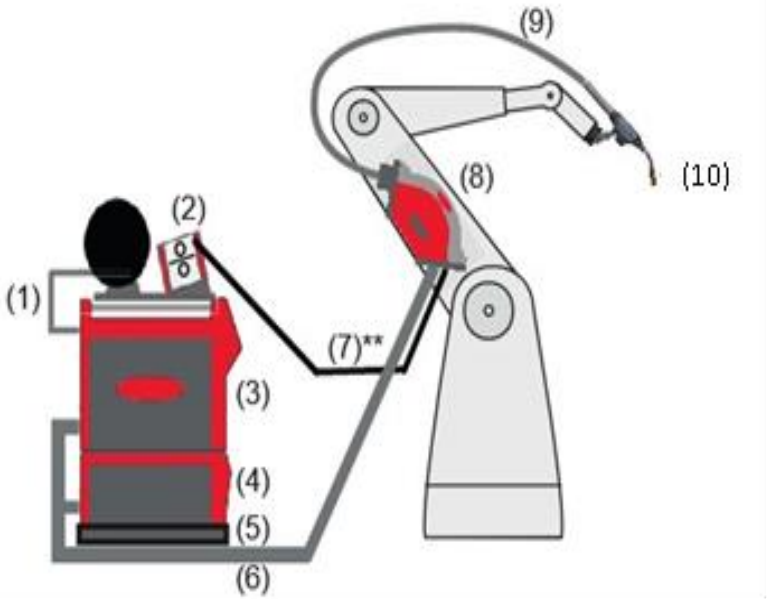

(1) Cable
(2) Dispenser
(3) Power source
(4) Cooling system
(5) Fixed base
(6) Wiring harness
(7) Dispenser and wire guide sleeve
(8) SplitBox
(9) Welding torch cable assembly
(10) Robot welding torch

Fig. 1. Description of a CMT equipment

Previous studies have shown the impact of Travel Speed (TS), shielding gas and WFS on bead geometry [10]. Wang et al, performed variations of different welding parameters such as laser power, laser beam size, ratio between arc and laser, TS, and WFS to understand their influence on weld bead geometry [11]. Wani et al. proposed examining the impact of TS and WFS parameters on the geometry of multi-layer deposition. From their studies, the power of the heat source, WFS, and TS are identified to have an impact on the shape of single and multilayer beads. Although, WFS has been reported to be the most influential parameter in controlling the supplied heat input to the structure [12,13].

Modelling of WAAM processes can enable the anticipation of numerous phenomena that are difficult to observe or control experimentally. For instance, the optimization of experimental parameters to achieve good mechanical properties [14,15].

Furthermore, thermofluid models are particularly effective in predicting geometry, as they can highlight the sensitivity of parameters on deposited structure. These multiphysics models heavily rely on material properties and involve coupling multiple physical phenomena such as phase change, allowing for a detailed understanding of the process physics [14,15]. Studies on WAAM processes, have highlighted interesting results on the behaviour of molten pool, arc behaviour, and droplet dynamics [16,17]. The thermal history of fabricated structures by WAAM process can be modelled as reported by [17]. Cadiou et al. proposed a thermofluid model of droplets detachment of the deposited metal for several layers to predict the geometry and the thermal history of the workpiece.

Numerous studies have been conducted on the impact of CMT process parameters on the mechanical and thermal properties of deposited materials. However, no studies have been conducted on the identification and characterization of the deviation between the programmed and actual WFS on the generator. Therefore, this work will demonstrate the importance of controlling the WFS parameter as it has a significant impact on the bead geometry. A correction model based on the experiment will be proposed. Finally, a study using a thermofluid model will be applied to Ti-6Al-4V alloy. This work demonstrates that is possible to anticipate this parameter variation using the modelling and to correct it upstream of experiments in the future.

2. MATERIALS AND METHOD

Variation in the WFS parameter can be attributed to several factors such as the generator, wire feeder motor, wire friction, slippage, and CMT push-pull system. The wire feeder motor is composed of a toothed wheel that may induce wire slippage that could affect the WFS. To understand these variations, CMT processes that uses a push-pull system and TIG process will be investigated.

1.2 mm diameter CuAl and S460 steel wire were used for TIG and CMT process respectively. Figures 2 and 3 shows the setup of TIG process and CMT process respectively. Both processes feeder system feeding rate was calculated without arc-on by feeding the wire for a given period prior to the length measurement. Consequently, a trend curve was plotted by comparing the inputted WFS value on the generator with the calculated value. Similar tests were repeated with arc-on and selected TS was determined based on WFS/TS ratio.

Fig. 2. TIG setup

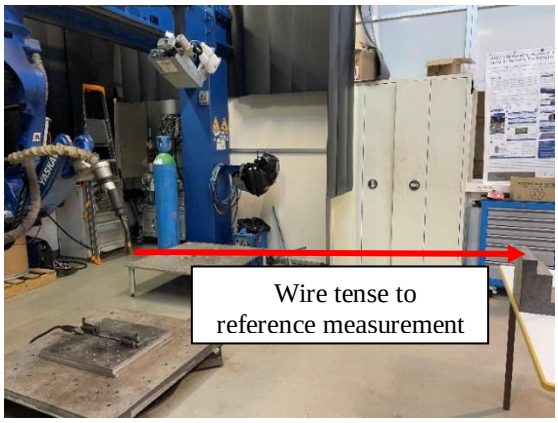

Fig. 3. CMT setup

A constant bead length of 125 mm was used and the deposition time (t_d) was calculated accordingly. The methodology of wire measurement prior to deposition is shown in Fig. 4. The theoretical length of wire to be consumed (L_{ThWC}) was calculated with the equation 1, and a reference value of 50 mm was added to the calculated value (L_{ThWC}) to get the total length of the wire (L_{Total}) as given in equation 2. After deposition, the remaining wire (W_r) was used to determine the amount of wire consumed (L_C) as shown in equation 3. (W_r) is designated positive when it is not less than the reference value, and vice-versa. The actual WFS (WFS_{actual}) is calculated from equation 4.

$$L_{ThWC} = WFS_I \times t_d \qquad (1)$$

$$L_{Total} = R_v + L_{ThWC} \qquad (2)$$

$$L_C = L_{Total} - W_r \qquad (3)$$

$$WFS_{actual} = \frac{L_C}{t_d} \qquad (4)$$

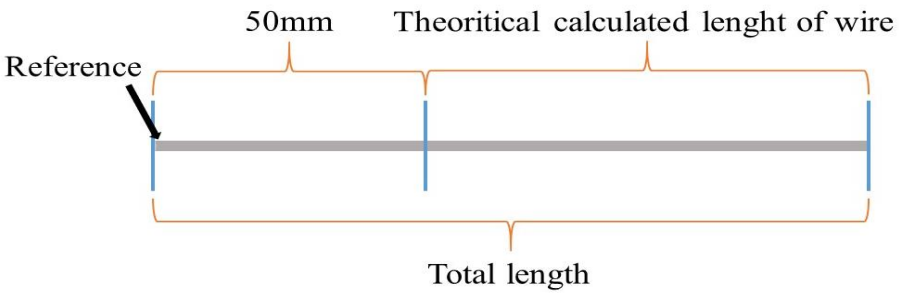

Fig. 4. Methodology of wire measurement

For TIG process, 9 trials were performed using a WFS values ranging from 2.0 to 2.5 m/min due to the allowable operating range. While that of CMT process, 18 trials were conducted comprising of 9 CMT and 9 CMT+P mode each. CMT being a high deposition rate process, a range of WFS values from 3 to 8 m/min were applied.

3. RESULTS AND DISCUSSION

3.1. EXPERIMENTAL RESULTS OF VARYING THE WFS PARAMETER:

For TIG trials without deposition and with CuAl deposition, two values of WFS were tested, 2, 2.3 and 2.5 m/min as presented in Table. 1 and 2 respectively. Each experiment was performed at least three times for repeatability. The calculated WFS values for TIG process without deposition showed a non-negligible difference from the inputted values, with an indicated error between 6.8% and 7.5%. Nevertheless, the tests with arc-on CuAl deposition had similar wire feed rates between the inputted and actual values.

Table 1. TIG experiment out of the process with CuAl wire

	WFS (m/min)	Feeding time (s)	Wire length measured (m)	Actual WFS (m/min)	Error %
Trial 1	2.0	30.22	0.93	1.85	7.5
Trial 3	2.3	30.31	1.08	2.14	7.0
Trial 2	2.5	30.42	1.18	2.33	6.8

Table 2. TIG experiment applied to CuAl deposition

	WFS (m/min)	TS (mm/min)	WFS/TS	Deposition time (s)	Consumed wire (m)	Actual WFS (m/min)	Error %
Trial 1	2.0	216	9.26	34.72	1.14	1.97	1.5
Trial 3	2.3	222	10.36	33.78	1.26	2.24	2.6
Trial 2	2.5	228	10.96	32.89	1.36	2.48	0.8

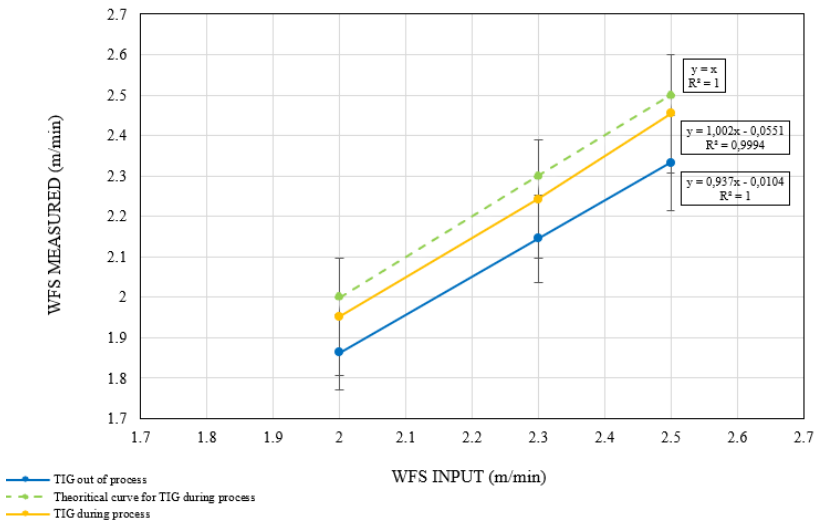

Fig. 5. Comparison between WFS input and measured in TIG

Figure 5 shows the comparison between the inputted and calculated WFS for TIG process. The test without deposition has a lower slope and an error of 5% margin as compared to the inputted value. This error could be due to the delay of the wire acceleration to attain the required speed.

For CMT experiments, the results are presented in Tables. 3 and 4. The inputted WFS values without deposition and with deposition was greater than the calculated values. The error values obtained for without deposition is within the range of 5.5–6.0%. While that of CMT deposition had an error within 3.1–12.0%. In the case of deposition, the percentage error decreases as the inputted WFS values increases.

Table 3. CMT experiments out of the process with Steel (S460) wire

	WFS (m/min)	Feeding time (s)	Wire length measured (m)	Actual WFS (m/min)	Error %
Trial 1	4.5	30.18	2.14	4.25	5.5
Trial 2	6.5	30.53	3.11	6.11	6.0
Trial 3	8.5	30.36	4.06	8.02	5.6

Table 4. CMT experiment apply to Steel (S460) deposition

	WFS (m/min)	TS (mm/min)	WFS/TS	Deposition time (s)	Consumed wire (m)	Actual WFS (m/min)	Error %
Trial 1	3.0	300	10.0	25.00	1.11	2.66	12.0
Trial 2	5.0	435	11.5	17.24	1.33	4.63	8.2
Trial 3	8.0	615	13.0	12.19	1.55	7.63	3.1

Table 5 presents the experimental value of CMT+P process. The error obtained ranges from 1.7–4.4%. Contrary, to CMT experiments, the calculated WFS values obtained were higher than the inputted values and the percentage error increases as the inputted values increases.

Table 5. CMT+P experiments apply to Steel (S460) deposition

	WFS (m/min)	TS (mm/min)	WFS/TS	Deposition time (s)	Consumed wire (m)	Actual WFS (m/min)	Error %
Trial 1	3.0	300	10.0	25.00	1.28	3.07	1.7
Trial 2	5.0	435	11.5	17.24	1.49	5.18	2.8
Trial 3	8.0	615	13.0	12.19	1.67	8.22	4.4

Figure 6, highlights the obtained results as the plotted curves are linear. The curve of CMT without welding and with deposition are closer in values and trends. However, a distinct difference is observed when compared with the CMT+P curve. The curves evolution are linear, thus allow for the establishment of a corrective model. This model, can correct the percentage error obtained between inputted and calculated WFS values.

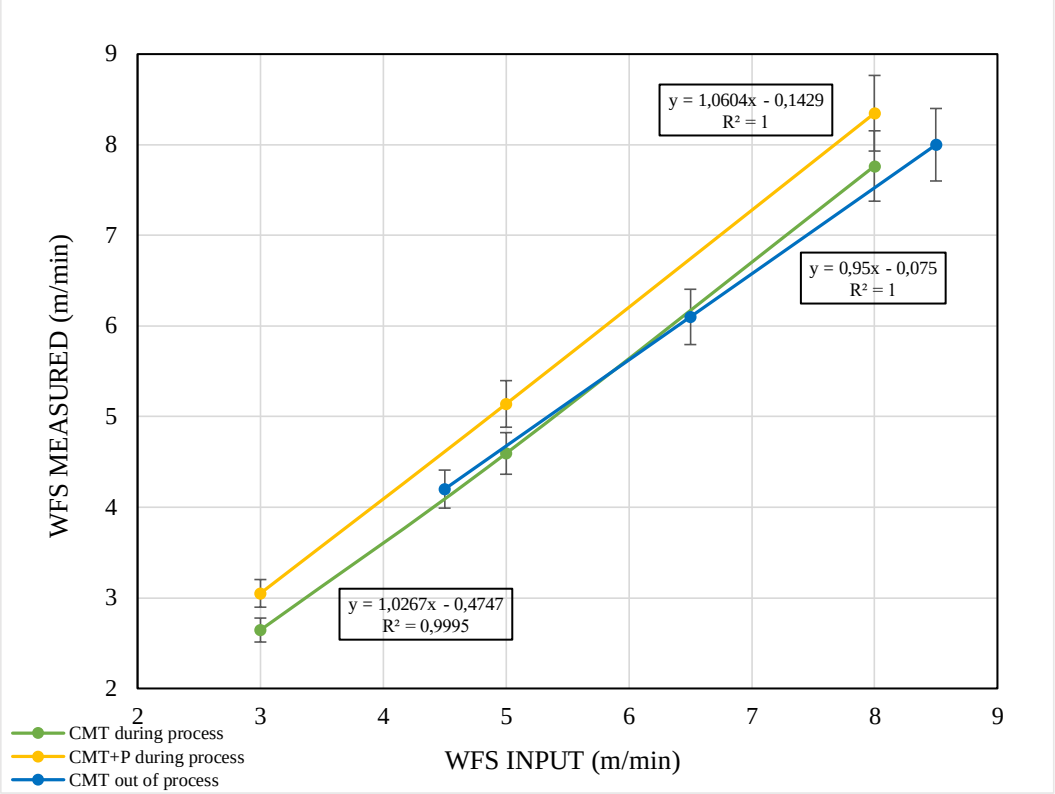

Fig. 6. Comparison between WFS input and measured in CMT

3.2. EFFECT OF WFS VARIATION ON BEAD GEOMETRY

Geometric measurements were carried out on each bead sample in terms of height and width using a venier caliper. The calculations of the bead cross-sectional areas were performed based on the measurements of height and widths for each sample. Figure 7 illustrates the results for CMT and CMT+P of WFS values of 3, 5, and 8 m/min. The WFS value has significant impact on the bead geometry [10–11]. Furthermore, the cross-sectional areas are larger as the WFS increases, especially that of CMT+P transfer mode.

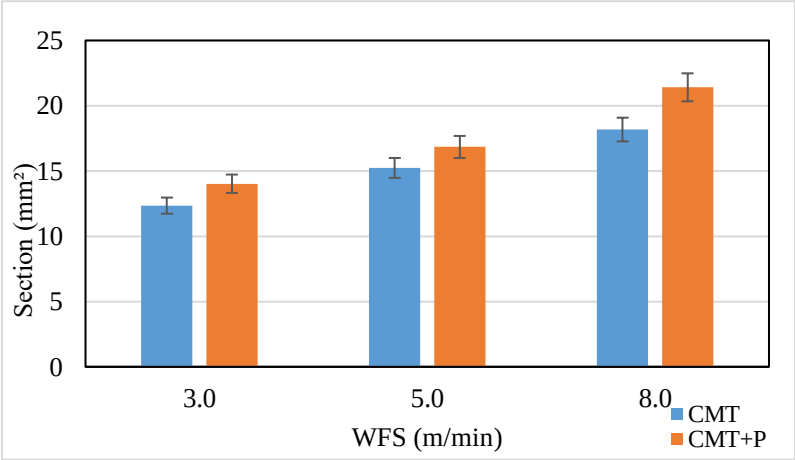

Fig. 7. Bead section results for CMT and CMT+P, S460

3.3 THERMOFLUID MODELISATION COMPARISON

Thermofluid modelisation of the WAAM process is based on several physics as fluid mechanics, thermal phenomena, and phase change. Several assumptions were made to build the model :

1. Shrinkage dynamics of wire and droplets are disregarded.
2. The fluid flow of gas and metal phases is assumed to be incompressible, immiscible, laminar, and Newtonian.
3. Arc plasma is in local thermodynamic equilibrium (LTE), with neglect of electron transfer enthalpy.
4. Arc plasma follows a Gaussian heat distribution.
5. The electromagnetic effects of the arc are considered negligible as compared to other forces.
6. Wire and heat source are assumed to be perfectly coaxial. Boundary conditions vary based on the side and are applied on all faces of the outer block.

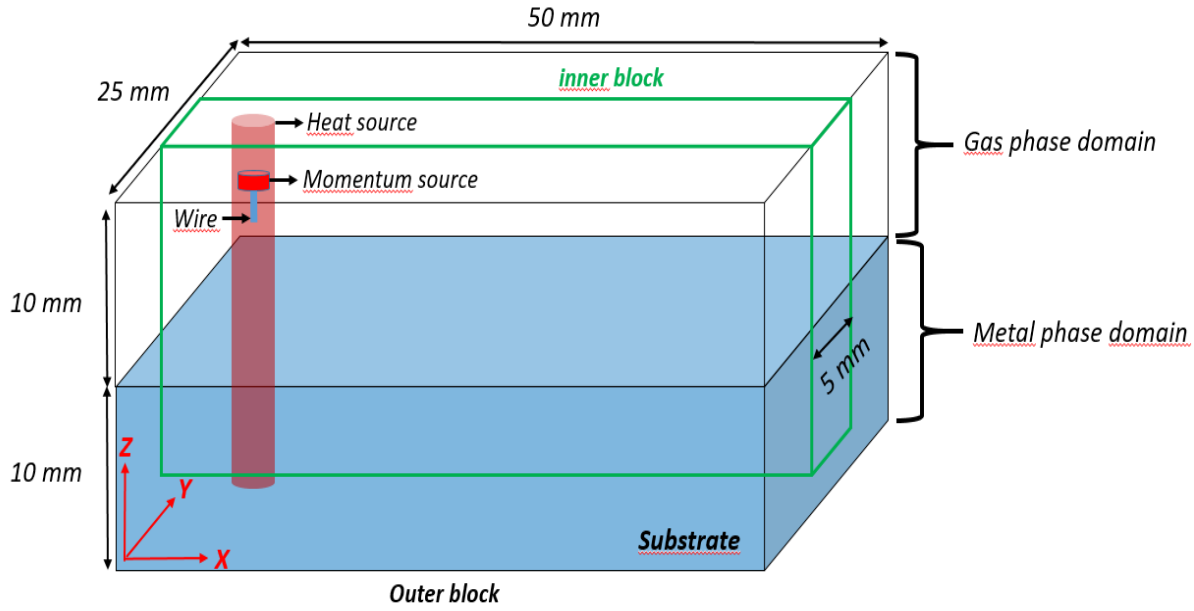

Fig. 8. Schematic of the computational domain

A computational domain is made of solid block with dimensions of 50 mm × 25 mm × 20 mm as depicted in Fig. 8, which is divided into zones: an upper zone filled with shielding gas and a lower zone representing the metal region. To enhance computational efficiency, the domain is discretised into non-uniform cubic blocks, with the innermost block positioned in the center as the area of interest. This inner block contains a fine mesh to provide a more realistic representation of temperature gradients and velocity. Surrounding the inner block is a second block with coarser mesh. The wire feed, represented by a momentum source is coaxial with the heat source and both must move simultaneously as constitutive components of the torch.

The boundary conditions presented in Table 6 are based on these six assumptions and are applied on all faces of the outer block.

Table 6. Boundary conditions

Boundary	Energy	Momentum
All outer block faces except Zmax,	$T = 293K$	$\vec{V} = \vec{0}$
Zmax outer block, specified pressure	$T = 293K$	$P \cdot \vec{n} = P_{atm} \cdot \vec{n}$
Inner block faces except Zmax,	ΔT	$\vec{V} = \vec{0}$
Zmax inner block, specified pressure	$T = 293K$	$P = P_{atm}$
Heat source	ΔT	$V = TS$
Momentum source	ΔT	$V = TS$
Flow rate	ΔT	$V = WFS$
Shield Gas	ΔT	$P = P_{arc}$

Deposits in Ti-6Al-4V alloy were made using CMT and CMT+P. The parameters used in the experimental phase as given in Table 7 were applied in the thermofluid model described above.

Table 7. Process parameter for CMT and CMT+P

N°	Travel speed (mm/min)	Wire feed speed (m/min)	WFS/TS
1-CMT	320	8.0	25
2-CMT	400	6.0	15
3-CMT+P	320	8.0	25
4CMT+P	240	6.0	15

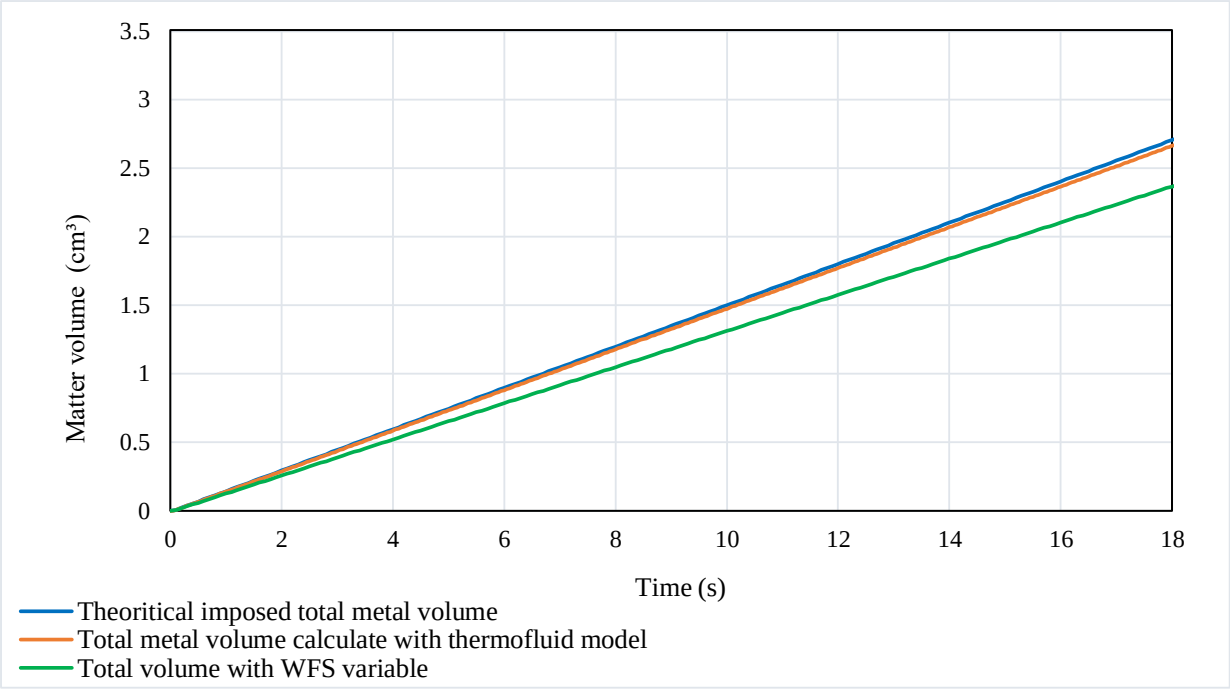

Fig. 9. WFS impact on metal volume theoritical and with thermofluid modelisation

Based on this set of parameters, a preliminary calculation of the theoretical and simulated volume of the deposited bead were conducted as illustrated in Fig. 9. These curves demonstrate that the volume of material produced by thermofluid model corresponds to the theoretical value. Therefore, the results validates the use of this model.
Initial trials were conducted with the WFS values indicated in Table 8. However, the simulated deposited beads cross-sectional areas did not correspond to the experimental sections, as shown in Fig. 10, with a percentage error of 15.7%.

The green curve depicted in Fig. 9, illustrates the significant impact of the flow rate on the matter volume produced by the thermofluid model. The flow rate, which is a function of WFS and wire diameter, has been identified as the factor responsible for the 15.7% difference between the simulated and experimental sections. Since the wire diameter is constant, the hypothesis suggests a potential variation in the WFS parameter.

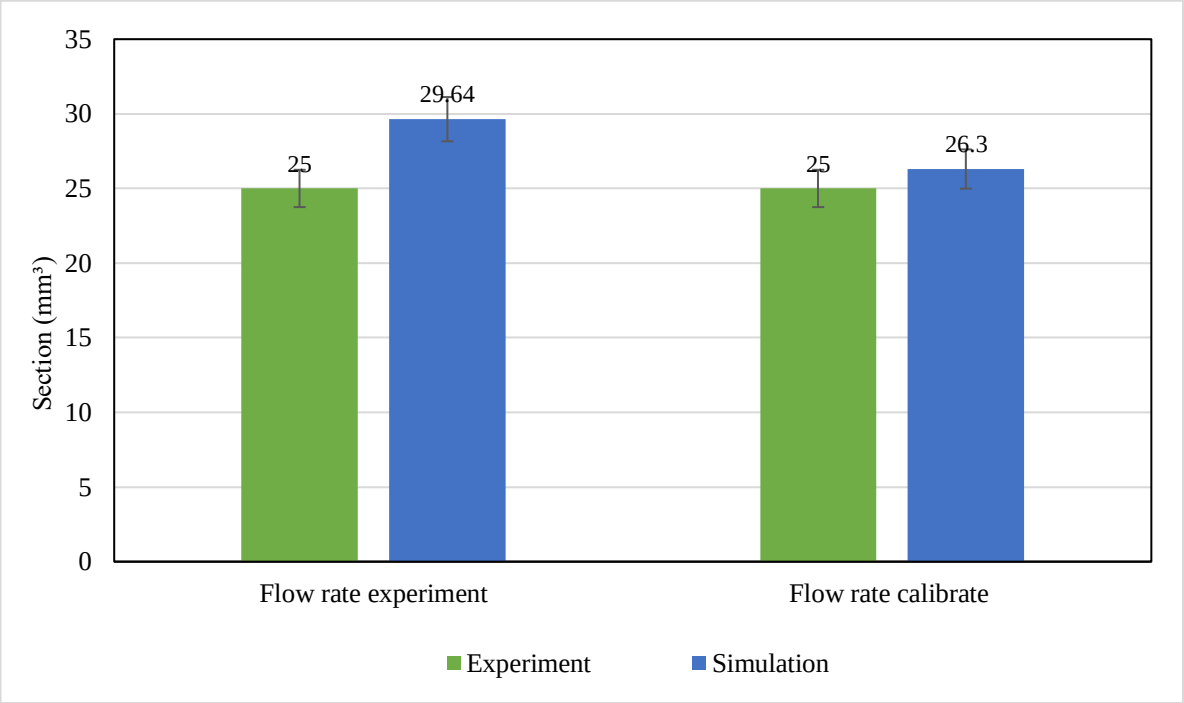

Fig. 10. Bead 1 section comparison between experiment and simulation

To assess the impact of WFS on the flow rate, various WFS values were examined from the graph shown in Fig. 9. Subsequently, a flow rate calibration was conducted with the following parameters: wire diameter (1.2 mm), WFS (7 m/min), and flow rate (0.13 cm^3/s) to correlate the simulated sections with the experimental ones.

The area of the cross-sections shown in Fig. 11, were calculated by multiplying the width and the height of the bead. Due to this calibration, the percentage error was reduced to 5.0% as compared to 15.7% without flow rate calibration, as shown in Fig. 10. These results shown in Fig. 11 demonstrate a precise response of the model with the calibrated WFS parameter.

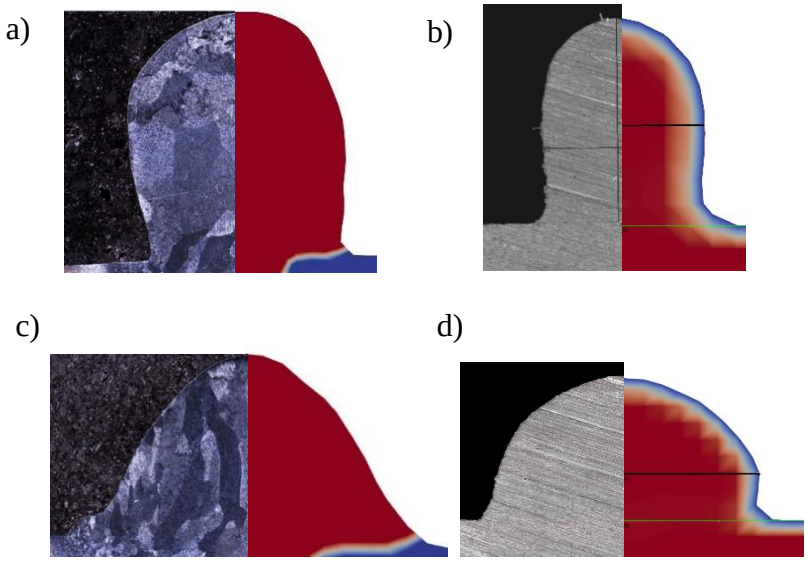

Fig. 11. Comparison of bead cross-section between experiment and simulation, a) sample 1; b) sample 2; c) sample 3; d) sample 4

4. CONCLUSION

This study investigated the impact of WFS parameter variation on experimental and simulation bead geometry. The main findings are as follows:

1. CMT and CMT+P process had significant variation in actual WFS as compared to inputted value, which could be related to the wire retraction configuration of both processes.
2. The study has revealed a significant correlation between the wire feed speed (WFS) parameter and the geometry of deposited beads.
3. The implementation of flow rate calibration reduced the cross-section discrepancy between simulated and experimental results. Therefore, demonstrating the effectiveness of the thermofluid model in predicting and correcting parameter variation.
4. These results offer promising prospects for precise optimization of Additive manufacturing parameters, thereby contributing to the improvement of weld quality and the efficiency of additive manufacturing processes by WAAM.

REFERENCES

[1] WU B., PAN Z., DING D., CUIRUI D., LI H., XU J., NORRISH J., 2018, *A Review of The Wire Arc Additive Manufacturing of Metals: Properties, Defects and Quality Improvement*, Journal of Manufacturing Processes, 35(July), 127—139.

[2] RAUCH M., DORADO J.P., HASCOET J.Y., RUCKERT G., 2021, *A Novel Method for Additive Manufacturing of Complex Shape Curved Parts by Using Variable Height Layers*, Journal of Machine Engineering, 21/3, 80–91.

[3] SHAH A., ALIVEV R., ZEIDLER H., KRINKE S., 2023, *A Review of the Recent Developments and Challenges in Wire Arc Additive Manufacturing (WAAM) Process,* Journal of Manufacturing and Materials Processing, 7/3, 97.
[4] RAUCH M., NWANKPA V.U., PECHET G., RUCKERT G., 2022, *A Methodology for Large Parts Wire and Arc Additive Manufacturing- a Ship Propeller Blade as Case Study*, American Journal of Engineering, Science and Technology (AJEST) 14, 32–41.
[5] Li J.L.Z., ALKAHARI M.R., ROSLI N.A.B., HASAN R., SUDIN M.N., RAMLI F R., 2019, *Review of Wire Arc Additive Manufacturing for 3D Metal Printing*, International Journal of Automation Technology, 13/3, 346–353.
[6] ARTAZA T., SUAREZ A., VEIGA F., BRACERAS I., TABERNERO I., LARRANAGA O., LAMIKIZ A., 2020, *Wire Arc Additive Manufacturing Ti6Al4V Aeronautical Parts Using Plasma Arc Welding: Analysis of Heat-Treatment Processes in Different Atmospheres*, JMRT, 9/6, 15454–15466.
[7] SRINIVASAN D., SEVVEL P., SOLOMON I.J., TANUSHKUMAAR P., 2022, *A Review on Cold Metal Transfer (CMT) Technology of Welding*, Selection and peer-review under responsibility of the scientific committee of the International Conference on Advanced Materials for Innovation and Sustainability, 04, 016.
[8] PRADO-CERQUEIRA J.L., DIEGUEZ J. L., CAMACHO A. M., 2017, *Preliminary Development of a Wire and Arc Additive Manufacturing System (WAAM)*, Procedia Manufacturing, 13, 895–902.
[9] Fronius, *Cold Metal Transfer: The technology, CMT technology*, www.fronius.com, 2023.
[10] DINOVITZER M., CHEN X., LALIBERTE J., HUANG X., FREI H., 2019, *Effect of Wire and Arc Additive Manufacturing (WAAM) Process Parameters on Bead Geometry and Microstructure*, Additive Manufacturing, 26, 138–146.
[11] WANG C., SUDER W., DING J., WILLIAMS S., 2021, *Bead Shape Control in Wire Based Plasma Arc and Laser Hybrid Additive Manufacture of Ti-6al-4v,* Journal of Manufacturing Processes, 68/PA, 1849–1859.
[12] WANI Z.K., ABDULLAH A.B., JAAFAR N.A., HUSSAIN Z., 2022, *Multi-Stages, Multi-Responses Optimisation of Wire Arc Additive Manufacturing Parameters Using Taguchi Method*, Materials Today Proceedings, 66, 2660–2664.
[13] HEMACHANDRA M., MAMEDIPAKA R., KUMAR A., THAPLIYAL S., 2024, *Investigating the Microstructure and Mechanical Behavior of Optimized Eutectic Al–Si Alloy Developed by Direct Energy Deposition*, Journal of Manufacturing Processes, 110, 398–411.
[14] SAMPAIO R.F.V., PRAGANA J.P.M., BRAGANCA I.M.F., SILVA C.M.A., NIELSEN C.V., MARTINS P.A.F., 2023, *Modelling of Wire-Arc Additive Manufacturing – a Review,* Advances in Industrial and Manufacturing Engineering, 6, 100121.
[15] ZHAO W., TASHIRO S., MURPHY A.B., TANAKA M., LIU X., WEI Y., 2023, *Deepening the Understanding of Arc Characteristics and Metal Properties in GMAW-Based WAAM With Wire Retraction Via a Multi-Physics Model*, Journal of Manufacturing Processes, 97, 260–274.
[16] BAI X., COLEGROVE P., DING J., ZHOU X., DIAO C., BRIDGEMAN P., ROMAN HONNIGE J., ZHANG H., WILLIAMS S. 2018, *Numerical Analysis of Heat Transfer and Fluid Flow in Multilayer Deposition of PAW-Based Wire and Arc Additive Manufacturing*, International Journal of Heat and Mass Transfer, 124, 504–516.
[17] CADIOU S., COURTOIS M., CARIN M., BERCKMANS W., LE MASSON P., 2020, *3D Heat Transfer, Fluid Flow and Electromagnetic Model for Cold Metal Transfer Wire Arc Additive Manufacturing (Cmt-Waam)*, Additive Manufacturing, 36, 101-541.